Journal of Nuclear Materials 384 (2009) 103–108

Contents lists available at ScienceDirect

Journal of Nuclear Materials

journal homepage: www.elsevier.com/locate/jnucmat

Development of the tailored SiC/SiC composites by the combined fabrication process of ICVI and NITE methods

Kazuya Shimoda [a,*], Tatsuya Hinoki [a], Yutai Katoh [b], Akira Kohyama [a]

[a] Institute of Advanced Energy, Kyoto University, Gokasho Uji, Kyoto 611-0011, Japan
[b] Materials Science and Technology Division, Oak Ridge National Laboratory, P.O. Box 2008, Oak Ridge, TN 37831-6138, USA

ARTICLE INFO

Article history:
Received 2 August 2008
Accepted 21 October 2008

ABSTRACT

In order to improve the thermo-mechanical performances of SiC/SiC composite, process improvement and modification by the combination of nano-infiltration and transient eutectic-phase (NITE) method and chemical vapor infiltration (CVI) method were studied. Multilayered PyC/SiC fiber coating and matrix infiltration within fiber-tows were prepared with isothermal/isobaric CVI (ICVI) method and full-densification of SiC matrix was examined with NITE methods using four kinds of processing options. Applied pressure was useful for nearly-full matrix densification due to the promoting infiltration driving force of SiC nano-powder intra-fiber-tows, but simultaneously caused the sever degradation of fibers and interphase with fracture, resulting in lower strength. Increase of additives amount and additional polymer were effective ways for matrix densification by SiC nano-power infiltration intra-fiber bundles without pressure. Thermal conductivity was greatly improved with the decrease of matrix porosity. The tailoring of thermo-mechanical properties might be easily controlled by the SiC matrix porosity without process-induced fibers and interphases degradations.

© 2008 Elsevier B.V. All rights reserved.

1. Introduction

For nuclear applications in fusion reactor, continuous SiC fiber reinforced SiC matrix (SiC/SiC) composites are potential candidate regarding their physical and chemical properties and their stability under irradiation [1,2]. However, realization of the reactor will be strongly depend on optimization of SiC/SiC composites microstructure, particularly in regard to the materials and processes used for the fiber, interphase and matrix constituents [3]. Several fabrication processes for SiC matrix densification, such as chemical vapor infiltration (CVI), polymer impregnation and pyrolysis (PIP), reaction sintering (RS) method, etc. have been under investigation for more than 10 years [4–8]. In the previous Japan–US collaborative JUPITER and JUPITER-II programs for nuclear fusion materials study, it was revealed that highly-crystallized SiC/SiC composites using advanced oxygen free, near-stoichiometric and crystallized SiC fiber had excellent resistance against neutron exposure [9,10]. At this time, chemical vapor infiltration (CVI) method is the only method to densify matrix with the advance fiber that is free from second phase. Matrix densification techniques other than CVI have been paid much attention to for long-term structural applications [10,11]. SiC/SiC composites fabricated by CVI method usually contain 10–20 vol.% porosity and are not dense, resulting in low thermal and mechanical properties. Dense matrix with low porosity is also required for reducing the leakage of helium gas as a coolant gas in the reactor [12,13]. Recently, a new process called nano-infiltration transient eutectic-phase (NITE) process using SiC 'nano'-slurry infiltration technique and pressure-sintering has been developed which produces nearly-full dense matrix with well-crystallized SiC at a lower sintering temperature than usual SiC fabrication, i.e., higher than 2000 °C while protecting SiC fibers and interface after induced processing conditions in our group at Kyoto University [14–17]. Both, therefore, CVI method and NITE method are recognized as promising fabrication methods of advanced SiC/SiC composites for nuclear fusion reactor applications due to the capability to produce near-stoichiometric and highly-crystallized SiC matrix. However, these have different features each other. CVI has the advantage of excellent infiltration into the narrow region of the intra-fiber bundle, but has the difficulty to form dense matrix among fiber bundles. On the contrast, NITE can form dense matrix among fiber bundles easily. It can be expected that the fundamental characteristics, such as density and thermo-mechanical properties of SiC/SiC composites will be improved furthermore by combining these.

The purpose of this work is to determine the tailoring of thermo-mechanical properties of SiC/SiC composites by the combination of NITE method to CVI method produced low-dense SiC/SiC composites. For these purposes, the effects of NITE processing parameters on density, thermal and mechanical properties were investigated in details.

* Corresponding author. Tel.: +81 774 383465; fax: +81 774 383467.
E-mail address: k-simd@iae.kyoto-u.ac.jp (K. Shimoda).

0022-3115/$ - see front matter © 2008 Elsevier B.V. All rights reserved.
doi:10.1016/j.jnucmat.2008.10.025

2. Experimental procedure

2.1. Materials and fabrication procedure

Pyrolytic carbon (PyC) was usually used as the fiber and matrix (F/M) interface of SiC/SiC composites in nuclear fusion region. According to the previous reports, PyC was very sensitive to both irradiation and temperature [18,19]. Therefore, thinner PyC interlayer is desirable to reduce these damages [19]. Another is $(PyC/SiC)_n$ multilayered interphase, in which very thin PyC layers and thicker SiC layers are alternately stacked (by n times), is presently the most promising for SiC/SiC composites [20]. Multilayered PyC/SiC coated SiC/SiC composite used in this study was fabricated by isothermal/isobaric chemical vapor infiltration (ICVI) system at Hyper-Therm High-Temperature Composites, Inc. (Huntington Beach, CA, USA). Tyranno™-SA SiC fiber cloth woven in 90° crossing two-dimensions (Ube Industrials Ltd., Japan) was employed as the reinforcement. A typical cross-sectional FE-SEM images of as-received ICVI-SiC/SiC composites were shown in Fig. 1: (a) inter-fiber-tows, (b) intra-fiber-tows and (c) PyC/SiC multilayer interphase. Among the various CVI techniques, ICVI method is generally a slow deposition rate and easy control of interface/interphase technique but readily applicable to large and/or complex-shaped components. This concept was proposed for improved fracture behavior, oxidation/irradiation resistance and lifetime [20–22]. Test bars for mechanical properties and test cylinders for thermal properties were cut from as-received ICVI-SiC/SiC composite with dimensions of $4^{W} \times 2^{T} \times 25^{L}\,mm^3$ and of approximately 10 mm in diameter and 2 mm in thickness, respectively. The cut bars and cylinders were dipped in three kinds of SiC 'nano'-slurries: (i) the mixture of SiC nano-sized powder and standard processing additive content (SC), (ii) the mixture of SiC nano-sized powder and twice as standard processing additive content ($SC \times 2$), and (iii) the mixture of SiC nano-sized powder and standard processing additive content incorporating polycarbosilane (PCS) (SC + PCS). The details of raw materials and SiC 'nano'-slurries were described elsewhere [15,17,23,24]. These prepared SiC/SiC composite compacts were placed in carbon powder, and then hot-pressing at 1900 °C in Ar for 1 h under the pressure of 20 MPa (P20) or under the pressure-less (PL) by called pseudo-HIP process, using a carbon powder as the pressure transmitter.

2.2. Characterization of the SiC/SiC composites fabricated by the combination processes

Composite compacts with the additional of the different NITE methods were polished on their four sides to mirror surface with diamond slurry (nominal particle size 1–3 μm) for mechanical properties. Bulk density and open porosity of the composites was measured by the Archimedes' method, using distilled water as the immersion medium. Microstructural observation was carried out using digital microscope and field-emission scanning electron microscope (FE-SEM). Average bending strength, proportional limit stress (PLS) and apparent bending modulus of composites were measured by three-point bending test at room-temperature in air using an INSTRON 5581 test machine. The support span length was 18 mm and cross-head speed was 0.5 mm/min in this work. Bending strength was determined from the peak load on the load–displacement curve. For each process, number of specimens measured by three-point bending test was three. The thermal diffusivity and the heat capacity in the direction through the thickness were measured by laser flash technique at room-temperature in air using a TC7000 test machine (ULVAC-RIKO, Inc., Japan). The thermal diffusivity (α) was obtained by $t_{1/2}$ method [25]. The thermal conductivity (K) in the direction through the thickness was calculated from the thermal diffusivity, the specific-heat and the density of each SiC/SiC composites, using the following equation:

$$K = \alpha \rho C_v, \quad (1)$$

where α is the thermal diffusivity, ρ is the density and C_v is the specific-heat. For each process, number of specimens measured by thermal test was two. The obtained thermal and mechanical results were compared with those of ICVI-SiC/SiC composite without the combination of NITE method.

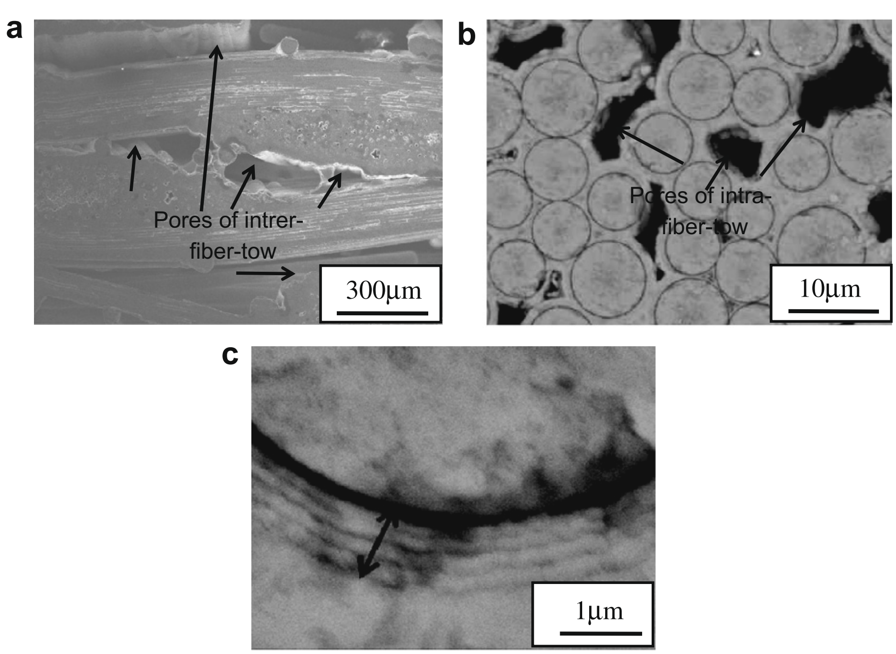

Fig. 1. FE-SEM images of as-received ICVI-SiC/SiC composites: (a) inter-fiber-tows, (b) intra-fiber-tows and (c) PyC/SiC multilayer interphase.

3. Results and discussion

3.1. Characterizations and microstructures

Table 1 shows bulk density, open porosity of ICVI-SiC/SiC composites and the SiC/SiC composites with the additional of different NITE methods. ICVI-SiC/SiC composites contained open porosity of about 18%, consisting of macro-pores (~hundreds microns in size) at inter-fiber-tows as mentioned (Figs. 1(a) and 2(a)). The PyC/SiC multilayer was approximately consisted of five layers (80 nm thickness for PyC layer on fiber surface, 20 nm thickness for PyC × 4 layers and 100 nm thickness for SiC sub-layers between PyC layers), as shown in Fig. 1(c). Bulk density was enhanced and open porosity was reduced on the SiC/SiC composites with the additional of SiC 'nano'-slurries infiltration. In addition, applied pressure during hot-pressing was effective way to increase bulk density and decrease open porosity furthermore. Fig. 2 shows digital images on surface and cross-section of ICVI-SiC/SiC composites and the SiC/SiC composites with the additional of different NITE methods. Surface of all composites with the additional of NITE methods were well-densified by SiC nano-crystal phase and large pores among fiber-tows were not detected. Large pores at center region of cross-section have a close relationship with bulk density. It was supposed that this may cause the highest density of ICVI + NITE (SC + P20) with applied pressure due to the promoting infiltration driving force of SiC nano-powder intra-fiber-tows.

3.2. Mechanical properties

Mechanical properties using three-point bending test are also summarized in Table 1 and typical bending stress–displacement curves were shown in Fig. 3. All composites fractured in non-brittle behavior. The average bending strength, PLS and apparent bending modulus of ICVI-SiC/SiC composites without the combination of NITE methods was about 250 MPa, 200 MPa and 50 GPa, respectively. ICVI + NITE (SC + P20) with the highest density showed lower average strength than ICVI-SiC/SiC composites without the combination of NITE methods and other composites with the combination of NITE methods. This supposed that too high applied pressure (20 MPa) for matrix densification caused the sever degradation of fibers and interphase with fracture at the center region of specimens is shown in Fig. 4. Without pressure, the average flexural strength and PLS have been improved with no sever degradations of fibers and interphase with fracture. In particular, the average strength of ICVI + NITE (SC × 2 + PL) was about twice (~500 MPa) as that of ICVI without the combination of NITE methods. PLS of ICVI + NITE (SC × 2 + PL) was not able to be measured because of no obvious elastic region. This result might be due to the poor crack propagation resistance caused by the reaction between PyC interphase and extra additional additives for matrix densification. Extra additional additives caused oxide segregations at triple points of SiC grains, as shown in Fig. 5. ICVI + NITE (SC + PCS + PL) exhibited higher average flexural strength (about 450 MPa) and fracture behavior with obvious elastic and pseudo ductile region. Fig. 6 shows fracture surfaces on cross-section after three-point bending test. Large pores, in particular, at inter-fiber-tows allow crack initiation and propagation easily. Meanwhile, a relative well-densified matrix without applied pressure would

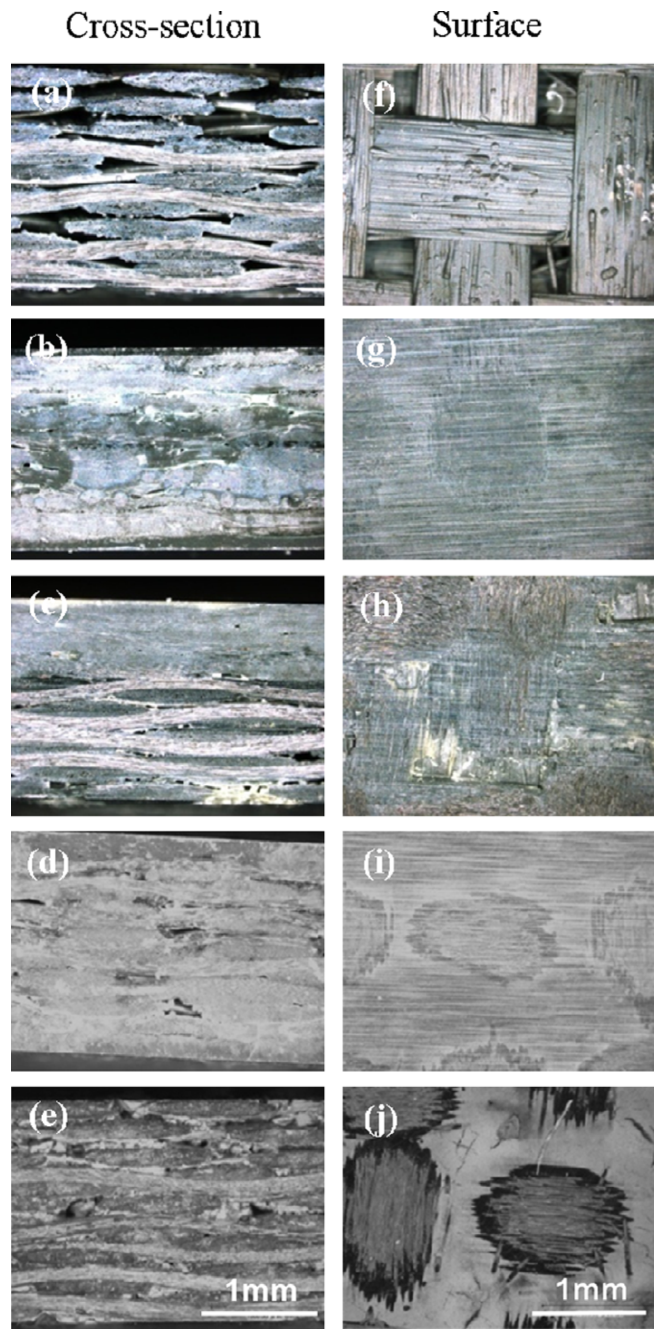

Fig. 2. Digital images on surface and cross-section: (a) and (f) ICVI, (b) and (g) ICVI + NITE (SC + P20), (c) and (h) ICVI + NITE (SC + PL), (d) and (i) ICVI + NITE (SC × 2 + PL) and (e) and (j) ICVI + NITE (SC + PCS + PL).

Table 1
Density, open porosity and mechanical properties from three-point bending.

Specimen ID	Bulk density (g/cm^3)	Open porosity (%)	Bending stress (MPa)	PLS[a] (MPa)	Elastic modulus (GPa)
ICVI	2.37	18	254 ± 8.1	200 ± 11	50.2 ± 2.1
ICVI + NITE (SC + P20)	2.96	3.7	152 ± 10	142 ± 15	117 ± 7.3
ICVI + NITE (SC + PL)	2.73	9.7	348 ± 18	259 ± 23	97.5 ± 4.5
ICVI + NITE (SC × 2 + PL)	2.87	5.0	497 ± 11	–	59.0 ± 5.0
ICVI + NITE (SC + PCS + PL)	2.83	5.9	442 ± 43	365 ± 28	106 ± 1.3

[a] PLS, proportional limit stress.

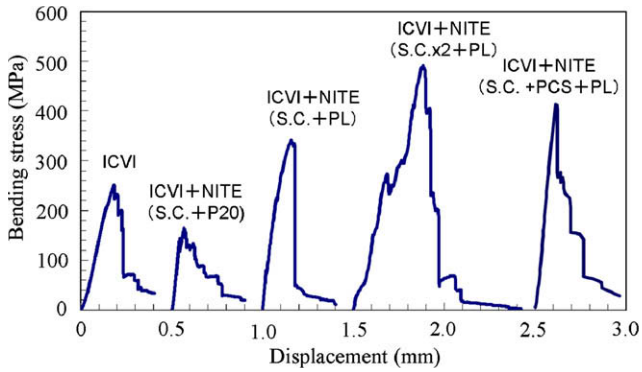

Fig. 3. Typical stress–displacement curves from three-point bending test.

hinder crack initiation and arrest crack propagation, resulting in higher PLS and apparent elastic modulus. From the additional of different NITE methods, matrix densification of inter-fiber-tows without fiber and interphase degradation could be considered as key technique for the enhancement of mechanical properties. However, since matrix densification of intra-fiber-tows will finally affect the crack initiation and propagation, the improvements of matrix densification of intra-fiber-tows will become be fundamental for future efforts.

3.3. Thermal properties

Fig. 7 shows the thermal conductivity of ICVI-SiC/SiC composites and the SiC/SiC composites with the additional of different NITE methods calculated from Eq. (1). Thermal conductivity of SiC/SiC composites will be strongly depend on SiC/SiC composites microstructure, particularly in regard to the materials and processes used for the fiber, interface and matrix constituent. It is known that recently developed SiC fibers, such as Tyranno™-SA and Hi-Nicalon™ Type S, have achieved higher fiber thermal conductivity than previous fibers, resulting in higher composites thermal conductivity using their fibers [26,27]. A lot of efforts for the improvement of low thermal conductivity have been emphasized on the decrease porosity in CVI based matrix. In this study, thermal conductivity of as-received ICVI-SiC/SiC composites has been enhanced and successfully improved with the combination of different NITE methods for matrix densification. As shown in Fig. 8, thermal conductivity of composites strongly depended on open porosity. The thermal conductivity of ICVI + NITE (SC + P20) with the highest density showed the highest in the SiC/SiC composites fabricated in this study, which were much higher than that of the conventional CVI-SiC/SiC composites [27]. However, thermal conductivities of ICVI + NITE (SC × 2 + PL and SC + PCS + PL) without applied pressure during hot-pressing was nearly the same or slightly higher compared with that of conventional CVI-SiC/SiC. This may be attributed to the SiC matrix, in particular the constituent phases of SiC matrix. In general, glassy phase exists in grain boundary of liquid phase sintered SiC like NITE-derived matrix, having a very lower thermal conductivity of less than 1 W/mK [28]. In our preliminary work, PCS-derived SiC fabricated at the same temperature of 1900 °C also had a lower thermal conductivity less than 5 W/mK. Furthermore, oxide remains and their compounds, such as yttrium aluminum garnet (YAG) derived from processing additives, also may have low thermal conductivity. As a consequence, these issues might be hampering the thermal conductivity of ICVI + NITE (SC × 2 + PL and SC + PCS + PL) in spite of the inclusion of high thermal conductivity fibers.

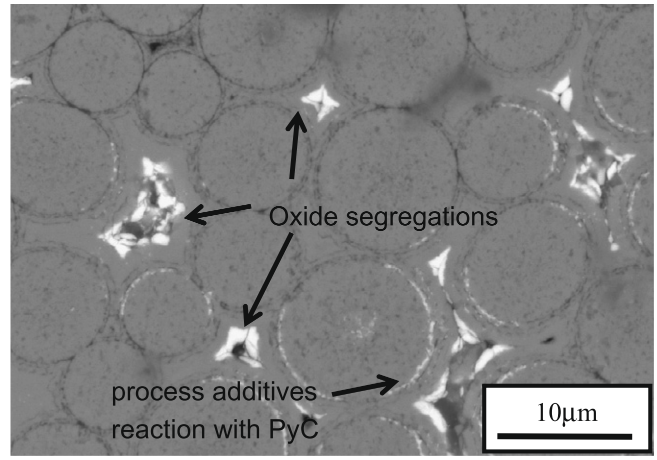

Fig. 5. FE-SEM images at intra-fiber-tows of ICVI + NITE (SC × 2 + PL).

By the additional of different NITE methods, densification of intra- and inter-fiber-tows was highly-achieved despite the insufficient process optimization. For high thermal conductivity, it is necessary to improve microstructures in matrix. Reduction of processing additives and PCS in additional of NITE methods leads to high thermal properties as well as irradiation resistance.

4. Summary

The tailoring of thermo-mechanical properties in SiC/SiC composites was investigated by developing the combination of NITE

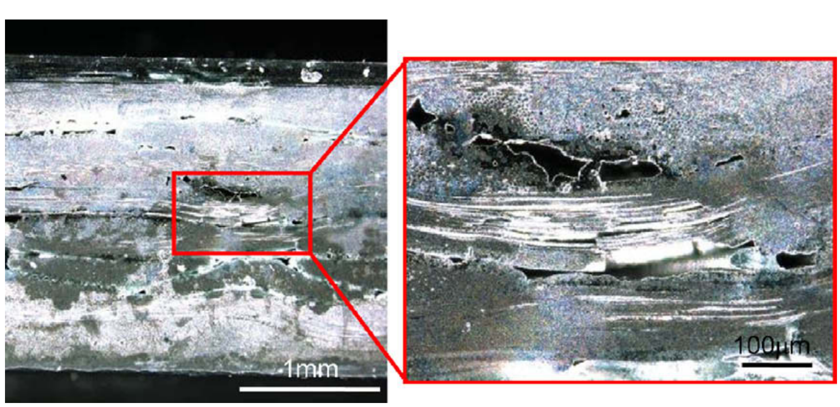

Fig. 4. Sever degradation of fibers and interphase with fracture at the center region of ICVI + NITE (SC + P20).

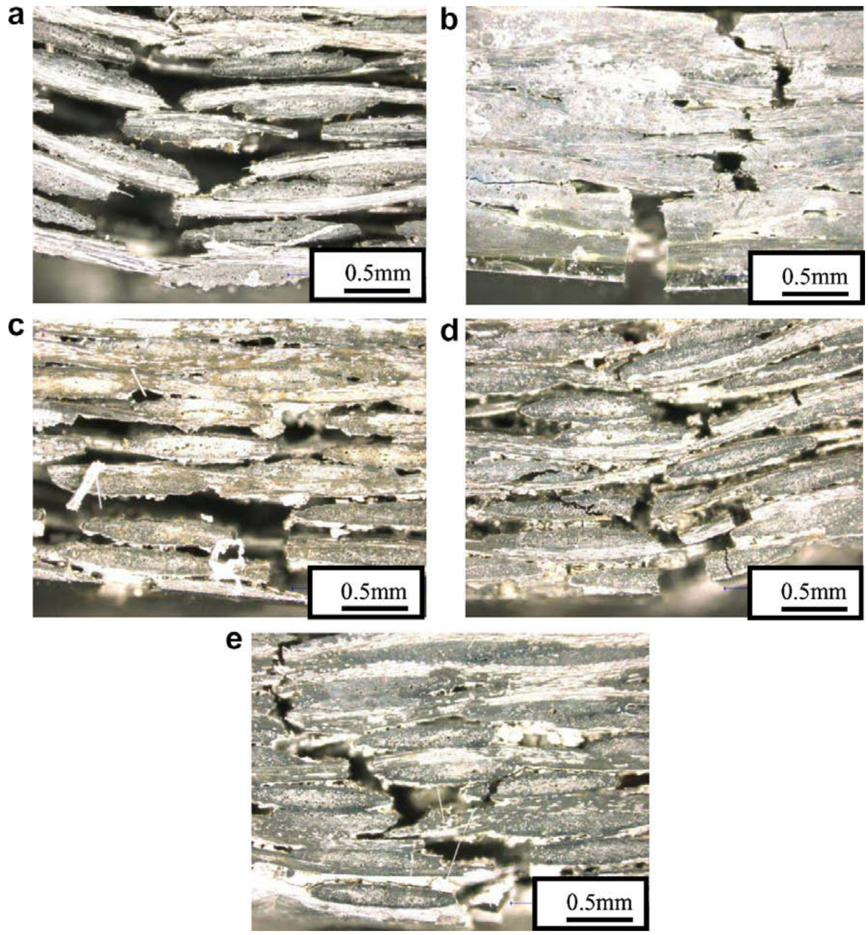

Fig. 6. Fracture surface on cross-section after three-point bending test: (a) ICVI, (b) ICVI + NITE (SC + P20), (c) ICVI + NITE (SC + PL), (d) ICVI + NITE (SC × 2 + PL) and (e) ICVI + NITE (SC + PCS + PL).

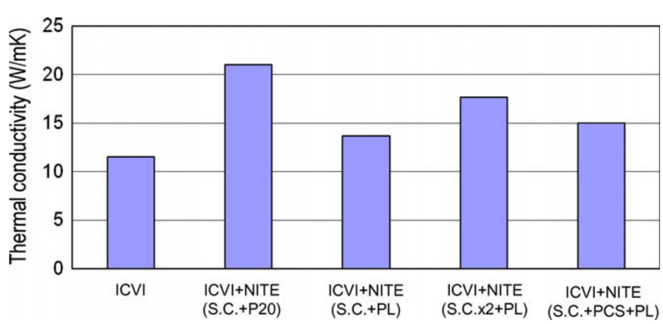

Fig. 7. Thermal conductivity in air at room-temperature.

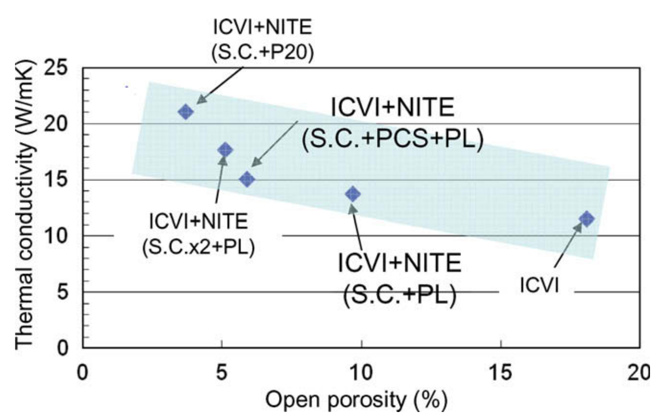

Fig. 8. Influence of the open porosity in SiC/SiC composites on thermal conductivity.

method to CVI method for the improvement of matrix porosity. For full-densification of ICVI-based SiC matrix, four kinds of NITE processing options were studied. Applied pressure was useful for matrix densification due to the promoting infiltration driving force of SiC nano-powder intra-fiber-tows, but simultaneously caused the sever degradation of fibers and interphase with lower strength. Increase of additives amount and additional polymer were effective way for matrix densification by the infiltration of SiC nano-powder at inter/intra-fiber-tows without pressure. Thermal conductivity was greatly improved with the decrease of matrix porosity. These studies clarified many useful processes with the selection of SiC 'nano'-slurry infiltration technique and applied pressure.

Acknowledgements

This research was partly sponsored by the 'JUPITER-II' US-Department of Energy/Japanese Ministry of Education, Culture, Sports, Science and Technology (MEXT) collaboration for fusion material system research.

References

[1] R.H. Jones, L. Giancarli, A. Hasegawa, Y. Katoh, A. Kohyama, B. Riccardi, L.L. Snead, W.J. Weber, J. Nucl. Mater. 307–311 (2002) 1057.

[2] R. Naslain, Compos. Technol. 64 (2004) 155.
[3] I.M. Low (Ed.), Ceramic Matrix Composites – Microstructure, Properties and Applications, Woodhead Publishing, Abington, England, 2006.
[4] R. Naslain, Adv. Compos. Mater. 8 (1999) 3.
[5] R. Naslain, Ceram. Trans. 144 (2002) 3.
[6] H. Araki, W. Yang, H. Suzuki, Q. Hu, C. Busabok, T. Noda, J. Nucl. Mater. 329–333 (2004) 567.
[7] M. Kotani, T. Inoue, A. Kohyama, K. Okamura, Y. Katoh, Compos. Technol. 62 (2002) 2179.
[8] A. Sayano, C. Sutoh, S. Suyama, Y. Itoh, S. Nakagawa, J. Nucl. Mater. 271–272 (1999) 467.
[9] T. Nozawa, T. Hinoki, L.L. Snead, Y. Katoh, A. Kohyama, J. Nucl. Mater. 329–333 (2004) 544.
[10] T. Nozawa, T. Hinoki, Y. Katoh, A. Kohyama, J. Nucl. Mater. 307–311 (2002) 1173.
[11] Y. Katoh, T. Nozawa, L.L. Snead, T. Hinoki, J. Nucl. Mater. 367–370 (2007) 774.
[12] S. Sharafat, R.H. Jones, A. Kohyama, P. Fenici, Fusion Eng. Des. 29 (1995) 411.
[13] T. Taguchi, N. Igawa, R. Yamada, S. Jitsukawa, J. Phys. Chem. Solids 66 (2005) 576.
[14] A. Kohyama, S.M. Dong, Y. Katoh, Ceram. Eng. Sci. Proc. 23 (2000) 311.
[15] S.M. Dong, Y. Katoh, A. Kohyama, J. Eur. Ceram. Soc. 23 (2003) 1223.
[16] Y. Katoh, A. Kohyama, T. Nozawa, M. Sato, J. Nucl. Mater. 329–333 (2004) 587.
[17] K. Shimoda, J.-S. Park, T. Hinoki, A. Kohyama, Compos. Technol. 68 (2008) 98.
[18] J.P. Singh, D. Singh, M. Sutaria, Composites A30 (1999) 445.
[19] Y. Katoh, L.L. Snead, T. Nozawa, T. Hinoki, A. Kohyama, N. Igawa, T. Taguchi, Mater. Trans. 46 (2005) 527.
[20] R. Naslain, Composites Part A 29A (1998) 1145.
[21] T. Nozawa, K. Ozawa, S. Kondo, T. Hinoki, Y. Katoh, L.L. Snead, A. Kohyama, J. ASTM Int. 2 (2005) 215.
[22] T. Hinoki, L.L. Snead, Y. Katoh, A. Kohyama, R. Shinavski, J. Nucl. Mater. 283–287 (2000) 376.
[23] K. Shimoda, J.-S. Park, T. Hinoki, A. Kohyama, Appl. Surf. Sci. 253 (2007) 9450.
[24] K. Shimoda, J.-S. Park, T. Hinoki, A. Kohyama, Ceram. Eng. Sci. Proc. 27 (2007) 207.
[25] W.J. Parker, R.J. Jenkins, C.P. Butler, G.L. Abbott, J. Appl. Phys. 32 (1961) 1679.
[26] R. Yamada, T. Taguchi, N. Igawa, J. Nucl. Mater. 283–287 (2000) 574.
[27] R. Yamada, N. Igawa, T. Taguchi, J. Nucl. Mater. 329–333 (2004) 497.
[28] W.D. Kingery, H.K. Bowen, D.R. Uhlman (Eds.), Introduction to Ceramics, second ed., Wilery, New York, 1976.